Dispersion and transport of microswimmers interacting with boundaries

Jean-Luc Thiffeault

Department of Mathematics
University of Wisconsin – Madison

joint with: **Hongfei Carrie Chen**

[Chen, H. & Thiffeault, J.-L. (2021). *J. Fluid Mech.* **916**, A15]

NSCCT20(+1)
Marseille virtuelle, 26 May 2021

WISCONSIN
UNIVERSITY OF WISCONSIN–MADISON

Microswimmer scattering off a surface

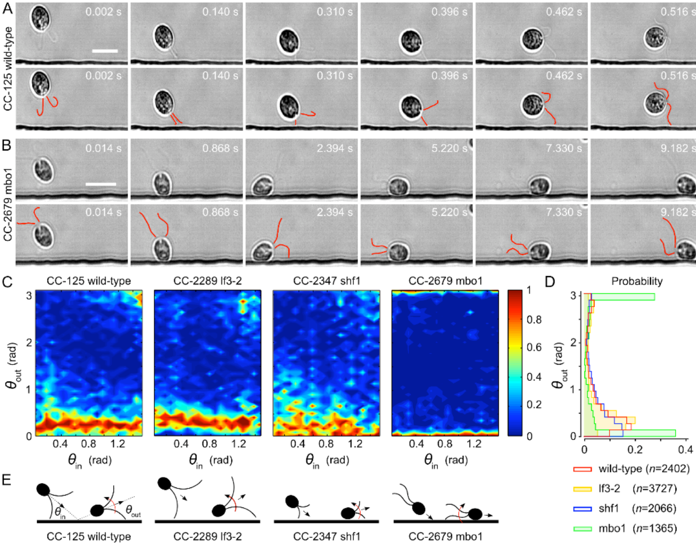

[Kantsler, V., Dunkel, J., Polin, M., & Goldstein, R. E. (2013). *Proc. Natl. Acad. Sci. USA*, **110** (4), 1187–1192]

play movie

Microswimmer scattering off a surface

- Large literature focusing on both steric and hydrodynamic interactions.
- Not always clear which one dominates.
- Here: focus on modeling steric interactions only, in particular the role of a microswimmer's shape.

See also

- Nitsche, J. M. & Brenner, H. (1990). *J. Colloid Interface Sci.* **138**, 21–41
- Contino, M., Lushi, E., Tuval, I., Kantsler, V., & Polin, M. (2015). *Phys. Rev. Lett.* **115** (25), 258102
- Spagnolie, S. E., Moreno-Flores, G. R., Bartolo, D., & Lauga, E. (2015). *Soft Matter,* **11**, 3396–3411
- Ezhilan, B. & Saintillan, D. (2015). *J. Fluid Mech.* **777**, 482–522
- Ezhilan, B., Alonso-Matilla, R., & Saintillan, D. (2015). *J. Fluid Mech.* **781**, R4
- Elgeti, J. & Gompper, G. (2015). *Europhys. Lett.* **109**, 58003
- Lushi, E., Kantsler, V., & Goldstein, R. E. (2017). *Phys. Rev. E,* **96** (2), 023102

The shape of a 2D swimmer

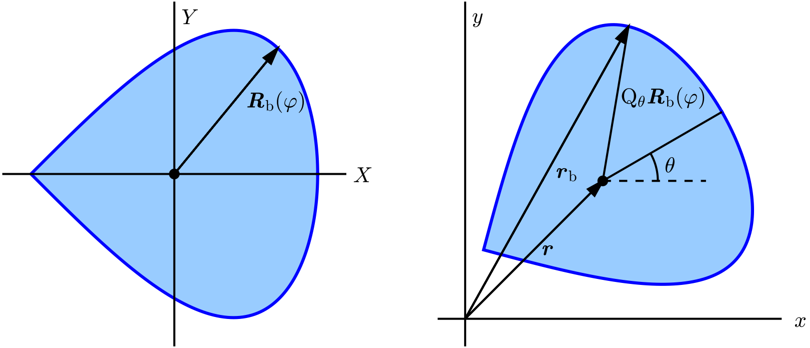

Convex swimmer in its frame (X, Y) and the fixed lab frame (x, y).

The swimming direction corresponds to $\varphi = 0$.

$\mathbb{Q}_\theta$ is a rotation matrix about a given center of rotation.

Swimmer touching a wall at $y = 0$

Denote by $y_*(\theta)$ the vertical coordinate of a swimmer with orientation θ when it touches the wall.

play movie

Convex swimmer touching a horizontal wall at $y = 0$:

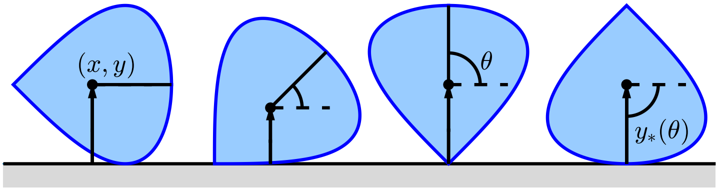

We call $y_*(\theta)$ the wall distance function. The swimmer's y coordinate must satisfy $y \geq y_*(\theta)$, otherwise the swimmer is inside the wall.

Wall distance function $y_*(\theta)$: needle

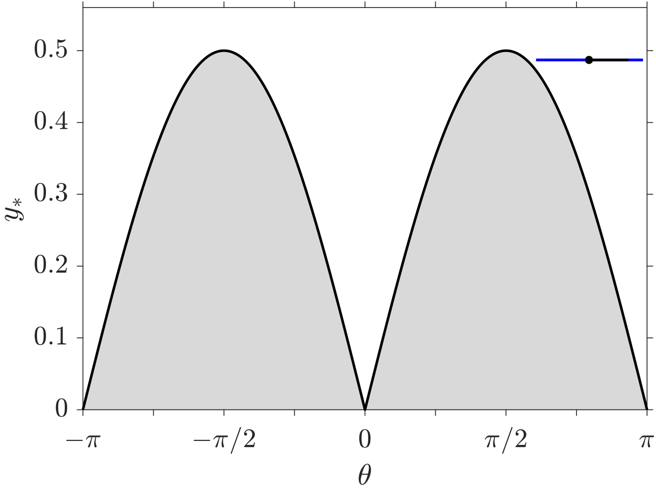

The needle has two corners; $y_*(\theta) = \frac{1}{2}\ell|\sin\theta|$

play movie

Wall distance function $y_*(\theta)$: off-center needle

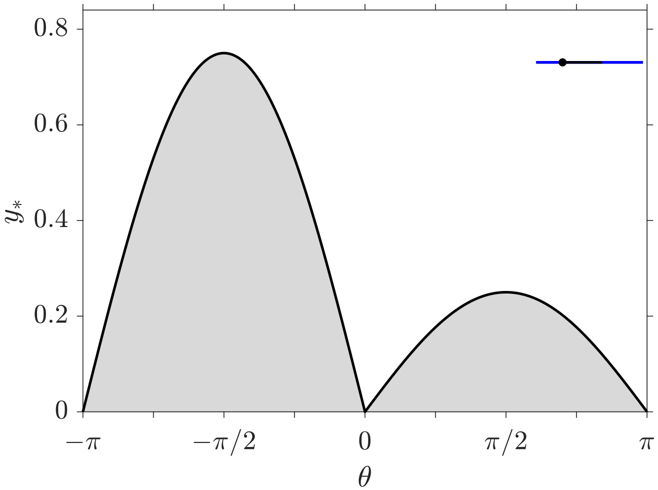

$$y_*(\theta) = \tfrac{1}{2}\ell|\sin\theta| - \tfrac{1}{4}\ell\sin\theta$$

play movie

Wall distance function $y_*(\theta)$: ellipse

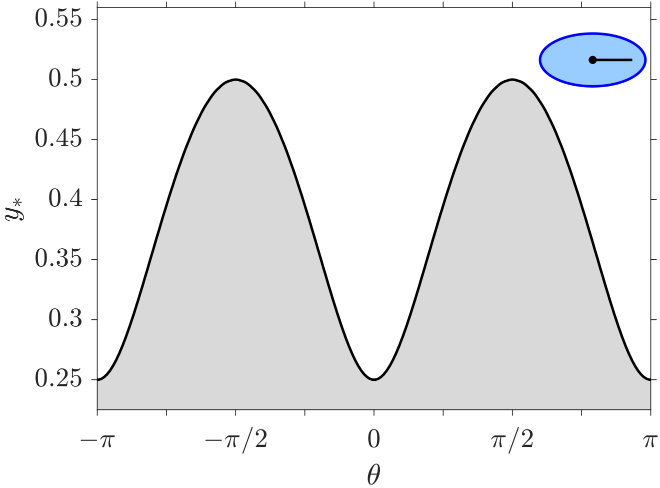

The ellipse has no corners; $y_*(\theta) = \sqrt{a^2 \sin^2\theta + b^2 \cos^2\theta}$

play movie

Wall distance function $y_*(\theta)$: off-center ellipse

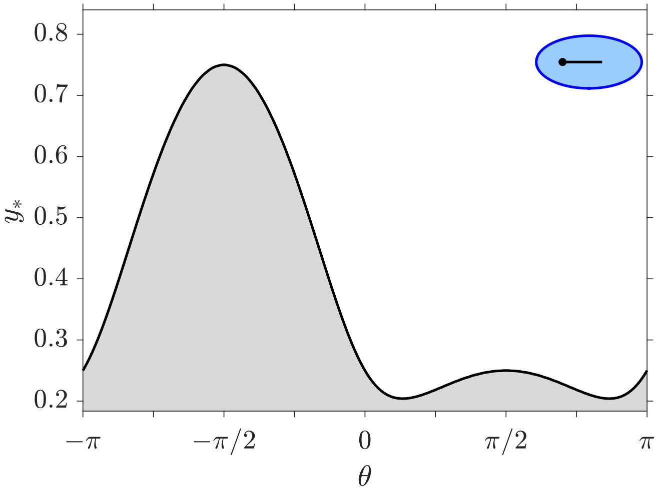

$$y_*(\theta) = \sqrt{a^2 \sin^2\theta + b^2 \cos^2\theta} - \tfrac{1}{2} a \sin\theta$$

play movie

Wall distance function $y_*(\theta)$: teardrop

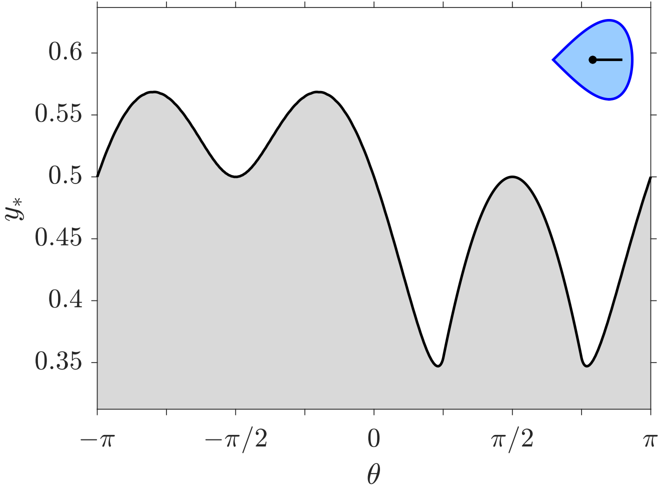

Teardrop has a corner and a smooth boundary. Local min at $\theta = -\pi/2$.

play movie

Reflection-symmetric swimmer

A swimmer with an axis of symmetry along its swimming direction has

$$\boxed{y_*(\theta) = y_*(\pi - \theta)}$$

that is, reflection-symmetry about $\pm\pi/2$.

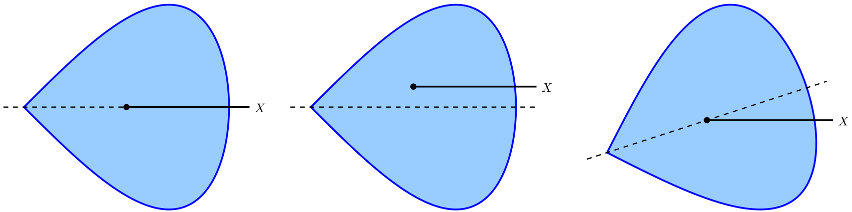

All the swimmers presented so far have that symmetry.

Easily broken by general shapes, but also by moving the center of rotation and direction of swimming.

A microswimmer in a channel

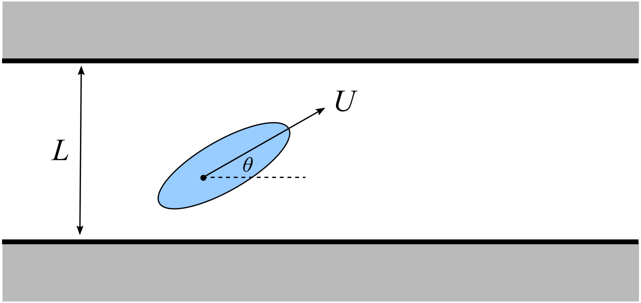

Channel geometry

So far we have considered only one wall.

For two parallel walls at $y = \pm L/2$, we have

$$\zeta_-(\theta) \leq y \leq \zeta_+(\theta)$$

where

$$\zeta_-(\theta) = y_*(\theta) - L/2, \qquad \zeta_+(\theta) = -y_*(\theta + \pi) + L/2.$$

$\zeta_\pm$ are related by the channel symmetry

$$\zeta_+(\theta) = -\zeta_-(\theta + \pi).$$

The channel symmetry is always satisfied, even for an asymmetric swimmer.

Open channel configuration space

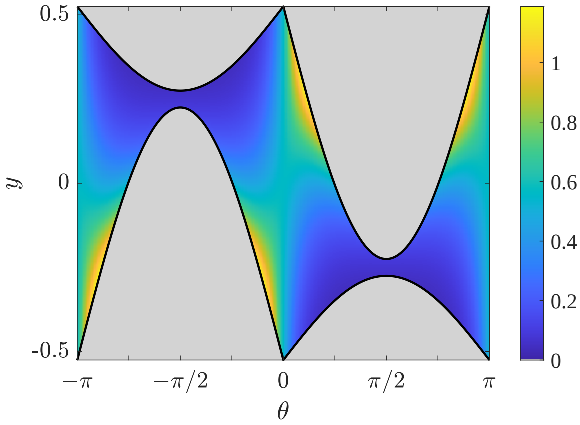

Configuration space for the needle in of length $\ell = 1$ in an open channel of width $L = 1.05$. (x not shown.)

A point in this space specifies the position and orientation of the swimmer.

Closed channel configuration space

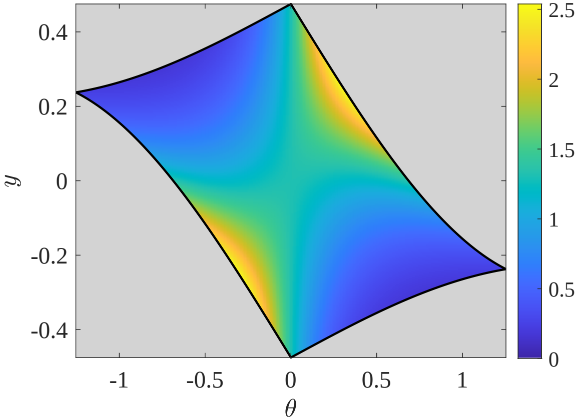

Configuration space for the needle in of length $\ell = 1$ in a closed channel of width $L = 0.95$.

The swimmer cannot reverse direction.

Stochastic model

The Brownian swimmer obeys the SDE

$$\begin{aligned} \mathrm{d}X &= U\,\mathrm{d}t + \sqrt{2D_X}\,\mathrm{d}W_1 \\ \mathrm{d}Y &= \sqrt{2D_Y}\,\mathrm{d}W_2 \\ \mathrm{d}\theta &= \sqrt{2D_\theta}\,\mathrm{d}W_3 \end{aligned}$$

in its own rotating reference frame.

In terms of absolute x and y coordinates, this becomes

$$\begin{aligned} \mathrm{d}x &= \left(U\,\mathrm{d}t + \sqrt{2D_X}\,\mathrm{d}W_1\right)\cos\theta - \sin\theta\,\sqrt{2D_Y}\,\mathrm{d}W_2 \\ \mathrm{d}y &= \left(U\,\mathrm{d}t + \sqrt{2D_X}\,\mathrm{d}W_1\right)\sin\theta + \cos\theta\,\sqrt{2D_Y}\,\mathrm{d}W_2 \\ \mathrm{d}\theta &= \sqrt{2D_\theta}\,\mathrm{d}W_3\,. \end{aligned}$$

Sample paths

- Swimmer swims a distance U/D_θ in a time $1/D_\theta$.
- Swimmer diffuses a distance $\sqrt{D_X/D_\theta}$ in a time $1/D_\theta$.
- $\mathrm{Pe}_{\theta,X} := \frac{U}{D_\theta} \Big/ \sqrt{\frac{D_X}{D_\theta}} = \frac{U}{\sqrt{D_\theta D_X}}$ measures the smoothness of the path.

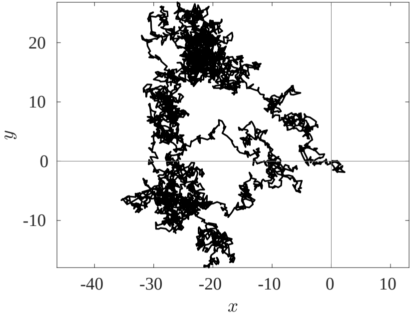

$\mathrm{Pe}_{\theta,X} \ll 1$

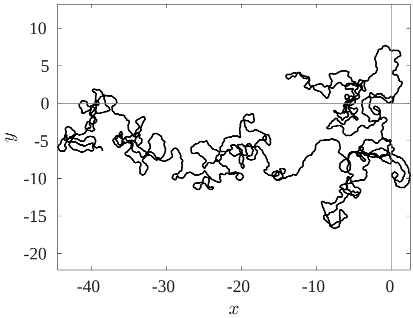

$\mathrm{Pe}_{\theta,X} \gg 1$

Fokker–Planck equation

The F–P equation for the probability density $p(x, y, \theta, t)$:

$$\partial_t p = -\nabla \cdot (\boldsymbol{u}\, p - \nabla \cdot \mathbb{D}\, p) + \partial_\theta^2 (D_\theta\, p)$$

where the drift vector and diffusion tensor are respectively

$$\boldsymbol{u} = \begin{pmatrix} U \cos\theta \\ U \sin\theta \end{pmatrix}$$

$$\mathbb{D} = \begin{pmatrix} D_X \cos^2\theta + D_Y \sin^2\theta & \frac{1}{2}(D_X - D_Y)\sin 2\theta \\ \frac{1}{2}(D_X - D_Y)\sin 2\theta & D_X \sin^2\theta + D_Y \cos^2\theta \end{pmatrix}.$$

Note that $\nabla := \hat{\boldsymbol{x}}\, \partial_x + \hat{\boldsymbol{y}}\, \partial_y$ (no θ).

How to handle the interaction of the swimmer with boundaries?

Volpe *et al.* (2014) use a specular reflection model (point swimmer):

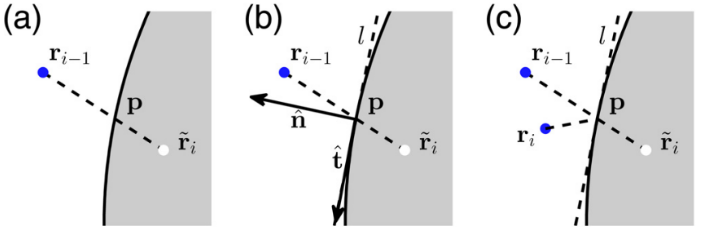

Fig. 3. Implementation of reflective boundary conditions. At each time step, the algorithm (a) checks whether a particle has moved inside an obstacle; if so: (b) the boundary of the obstacle is approximated by its tangent l at the point $\mathbf{p}$ where the particle entered the obstacle, and (c) the particle position is reflected on this line.

[Volpe, G., Gigan, S., & Volpe, G. (2014). *Am. J. Phys.* **82** (7), 659–664]

Boundary condition

For any fixed volume V we have

$$\partial_t \int_V p \,\mathrm{d}V = -\int_V \big(\nabla \cdot (\boldsymbol{u}\,p - \nabla \cdot (\mathbb{D}\,p)) - \partial_\theta^2 (D_\theta\,p)\big)\,\mathrm{d}V$$
$$= -\int_{\partial V} \boldsymbol{f} \cdot \mathrm{d}\boldsymbol{S}\,,$$

where ∂V is the boundary of V, and the flux vector is

$$\boldsymbol{f} = \boldsymbol{u}\,p - \nabla \cdot (\mathbb{D}\,p) - \hat{\boldsymbol{\theta}}\,\partial_\theta (D_\theta\,p).$$

Thus, on the reflecting (impermeable) parts of the boundary we require the no-flux condition

$$\boldsymbol{f} \cdot \boldsymbol{n} = 0, \quad \text{on} \quad \partial V_{\mathsf{refl}}$$

where $\boldsymbol{n}$ is normal to the boundary.

Configuration space and drift in θ–y plane

Drift is $U \sin\theta\,\hat{\boldsymbol{y}}$; no-flux condition forces swimmer to align with the wall.

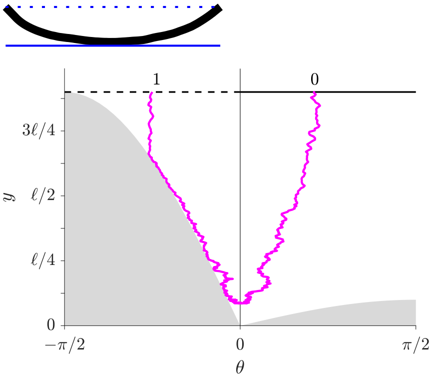

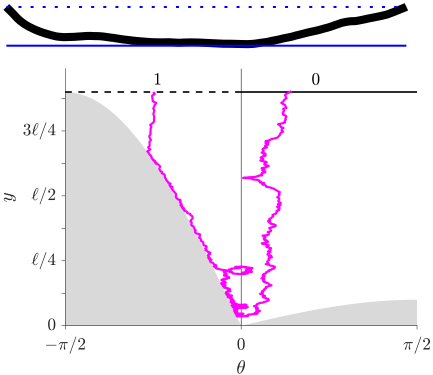

Once the particle crosses $\theta = 0$ (parallel to wall), it is pushed upward by the drift.

play movie

Reduced equation

The F–P equation is challenging to solve because of the complicated boundary shape.

Tractable limit $D_\theta \ll 1$ (small rotational diffusivity)

Get a (1+1)D PDE for $p(\theta, y, t) = P(\theta, T)\, \mathrm{e}^{\sigma(\theta) y}$

$$\partial_T P + \partial_\theta(\mu(\theta)\, P - \partial_\theta P) = 0, \qquad T \coloneqq D_\theta\, t,$$

$$\begin{aligned}
\sigma(\theta) &\coloneqq U \sin\theta / D_{yy}(\theta) \\
\mu(\theta) &\coloneqq \frac{\sigma(\theta)}{2\sinh\Delta(\theta)} \left(\mathrm{e}^{\Delta(\theta)}\, \zeta_+'(\theta) - \mathrm{e}^{-\Delta(\theta)}\, \zeta_-'(\theta)\right) \\
\Delta(\theta) &\coloneqq \tfrac{1}{2}\sigma(\theta)\,(\zeta_+(\theta) - \zeta_-(\theta)).
\end{aligned}$$

The shape of the swimmer enters through drift $\mu(\theta)$.

Invariant density and mean drift (open channel)

What is the natural invariant density $\mathcal{P}(\theta)$ for the swimmer? For open channel, 2π-periodic solution to

$$\partial_\theta(\mu(\theta)\,\mathcal{P} - \partial_\theta\mathcal{P}) = 0.$$

Integrate once:

$$\mu(\theta)\,\mathcal{P} - \partial_\theta\mathcal{P} = c_2.$$

Integrate this from $-\pi$ to π to find

$$\mathbb{E}\mu(\theta) = \int_{-\pi}^{\pi} \mu(\theta)\,\mathcal{P}\,\mathrm{d}\theta = 2\pi c_2 =: \omega.$$

ω is the mean drift or mean rotation rate of the swimmer.

Easy to show: if the swimmer is left-right symmetric, then $\omega = 0$ and the probability satisfies detailed balance.

An asymmetric swimmer thus picks up a mean rotation!

Invariant density examples: needle

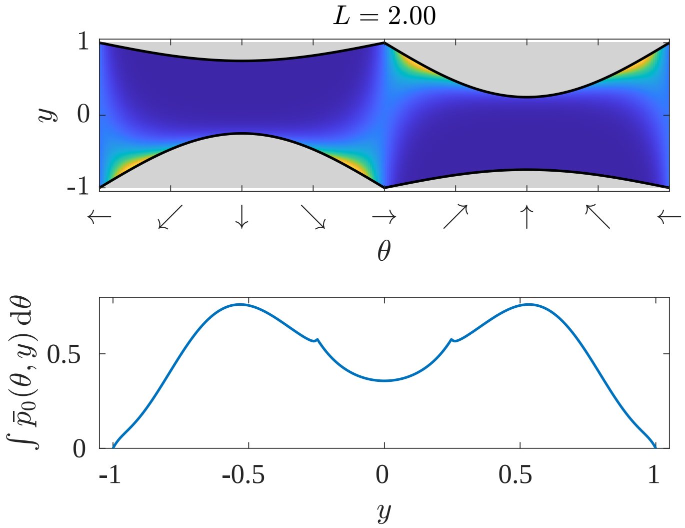

play movie

Invariant density examples: ellipse

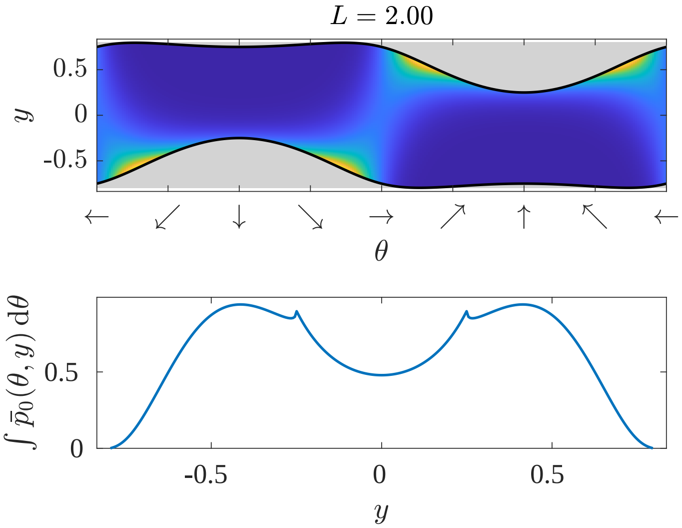

play movie

Invariant density examples: teardrop

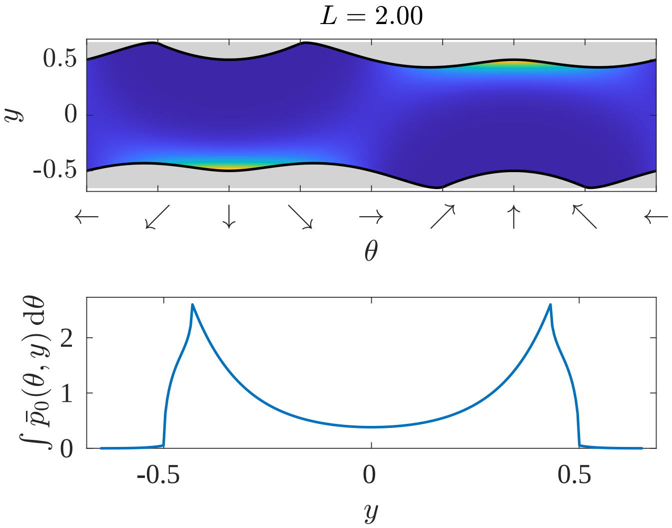

play movie

Mean exit time equation

From our reduced equation, we can derive an adjoint equation for the mean exit time of swimmer starting at orientation θ to reach the "exit" $\theta = \theta^{\mathrm{L}}$ or $\theta = \theta^{\mathrm{R}}$ for the first time:

$$\mu(\theta)\,\tau' + \tau'' = -1, \qquad \theta^{\mathrm{L}} < \theta < \theta^{\mathrm{R}};$$
$$\tau(\theta^{\mathrm{L}}) = \tau(\theta^{\mathrm{R}}) = 0.$$

The mean reversal time is the special case $\tau(0)$ for $-\theta^{\mathrm{L}} = \theta^{\mathrm{R}} = \pi$.

Expected time for the swimmer to completely reverse direction in the channel. [See Holcman & Schuss (2014) for the case without drift.]

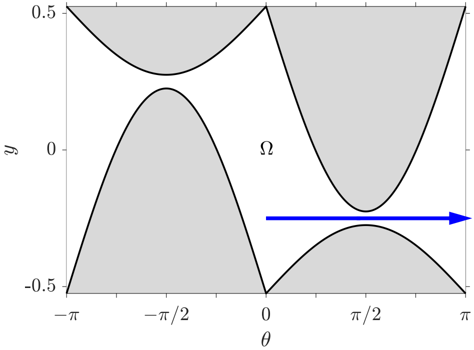

Mean reversal time

For a reflection-symmetric swimmer, the mean reversal time takes the simple form

$$\boxed{\tau_{\text{rev}} = \tfrac{1}{4}\int_0^{\pi} \frac{\mathrm{d}\vartheta}{\mathcal{P}(\vartheta)}}$$

where $\mathcal{P}(\theta)$ is the invariant density.

Intuitively, small $\mathcal{P}$ corresponds to "bottlenecks" that dominate the reversal time.

For the needle swimmer,

$$\tau_{\text{rev}} \approx \frac{\pi}{2\beta D_\theta}\,\mathrm{e}^{\beta}, \qquad \beta = U\ell/4D_Y\,.$$

From this we get an effective diffusivity

$$\boxed{D_{\text{eff}} \approx \tfrac{1}{2}\tau_{\text{rev}}\,U^2}$$

The diffusive needle

For a purely-diffusive ($U = 0$) needle of length ℓ in a channel of width L, the mean reversal time is

$$\tau_{\mathrm{rev}} = \frac{(\pi - 2\lambda)(\pi - \arccos\lambda)}{D_\theta\sqrt{1-\lambda^2}}, \qquad \lambda := \ell/L < 1.$$

The 'narrow exit' limit corresponds to $\lambda = 1 - \delta$, with δ small:

$$\tau_{\mathrm{rev}} = \frac{\pi(\pi - 2)}{D_\theta\sqrt{2\delta}} + \mathrm{O}(\delta^0), \qquad \delta \ll 1.$$

This is similar but not identical to [Holcman & Schuss (2014, Eq. (5.13))]:

$$\tau_{\mathrm{rev}}^{(\mathrm{HS})} = \frac{\pi(\pi - 2)}{D_\theta\sqrt{\delta}}\sqrt{\frac{D_X}{L^2 D_\theta}} + \mathrm{O}(\delta^0),$$

Our result holds for small D_θ, theirs for small δ.

Different scaling in D_θ! (Ours: D_θ^{-1}; theirs: $D_\theta^{-3/2}$.)

Numerical simulation of needle reversal

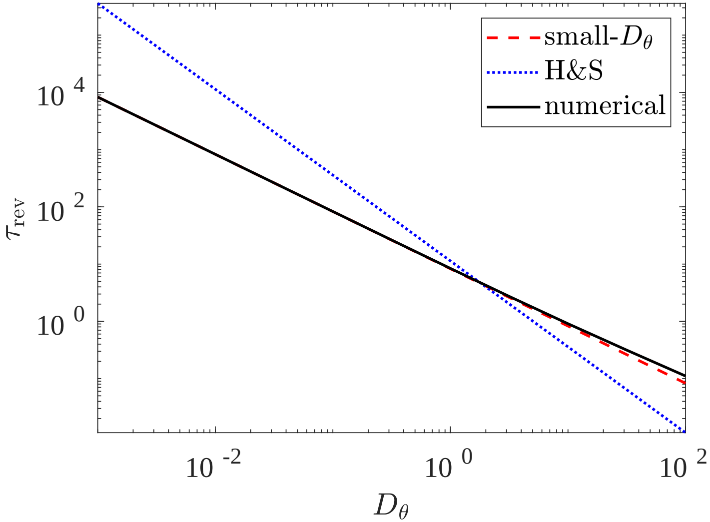

$U = 0,\ D_X = D_Y = 1,\ \lambda = 0.9,\ L = 1\ (\delta = 0.1)$

Discussion

- Simple model for a Brownian swimmer or interacting with walls.
- The boundary conditions are naturally dictated by conservation of probability in configuration space.
- Swimmer geometry plays a role as it affects the shape of configuration space.
- This opens up the analysis to PDE methods (Fokker–Planck equation).
- (1+1)D reduced PDE when y dynamics are fast compared to θ.
- Lots more to look at:
  - Effective diffusivity in terms of mean reversal time;
  - Scattering angle distribution;
  - 3D swimmers;
  - The $D_\theta \gg D_X$ limit (lots of boundary layers!);
  - Compare to experiments;
  - Other confined geometries.
- Chen, H. & Thiffeault, J.-L. (2021). *J. Fluid Mech.* **916**, A15

References I

Chen, H. & Thiffeault, J.-L. (2021). *J. Fluid Mech.* **916**, A15.

Contino, M., Lushi, E., Tuval, I., Kantsler, V., & Polin, M. (2015). *Phys. Rev. Lett.* **115** (25), 258102.

Elgeti, J. & Gompper, G. (2015). *Europhys. Lett.* **109**, 58003.

Ezhilan, B., Alonso-Matilla, R., & Saintillan, D. (2015). *J. Fluid Mech.* **781**, R4.

Ezhilan, B. & Saintillan, D. (2015). *J. Fluid Mech.* **777**, 482–522.

Holcman, D. & Schuss, Z. (2014). *SIAM Review,* **56** (2), 213–257.

Kantsler, V., Dunkel, J., Polin, M., & Goldstein, R. E. (2013). *Proc. Natl. Acad. Sci. USA,* **110** (4), 1187–1192.

Lushi, E., Kantsler, V., & Goldstein, R. E. (2017). *Phys. Rev. E,* **96** (2), 023102.

Nitsche, J. M. & Brenner, H. (1990). *J. Colloid Interface Sci.* **138**, 21–41.

Spagnolie, S. E. & Lauga, E. (2012). *J. Fluid Mech.* **700**, 105–147.

Spagnolie, S. E., Moreno-Flores, G. R., Bartolo, D., & Lauga, E. (2015). *Soft Matter,* **11**, 3396–3411.

Volpe, G., Gigan, S., & Volpe, G. (2014). *Am. J. Phys.* **82** (7), 659–664.